

# Elasticity solution and free vibrations analysis of laminated anisotropic cylindrical shells

M. Shakeri†, M.R. Eslami‡ and M.H. Yas††

*Department of Mechanical Engineering, Amirkabir University of Technology,  
Hafez Ave. No. 424, Tehran, Iran*

**Abstract.** Dynamic response of axisymmetric arbitrary laminated composite cylindrical shell of finite length, using three-dimensional elasticity equations are studied. The shell is simply supported at both ends. The highly coupled partial differential equations are reduced to ordinary differential equations (ODE) with variable coefficients by means of trigonometric function expansion in axial direction. For cylindrical shell under dynamic load, the resulting differential equations are solved by Galerkin finite element method, In this solution, the continuity conditions between any two layer is satisfied. It is found that the difference between elasticity solution (ES) and higher order shear deformation theory (HSD) become higher for a symmetric laminations than their unsymmetric counterpart. That is due to the effect of bending-stretching coupling. It is also found that due to the discontinuity of inplane stresses at the interface of the laminate, the slope of transverse normal and shear stresses aren't continuous across the interface. For free vibration analysis, through dividing each layer into thin laminas, the variable coefficients in ODE become constants and the resulting equations can be solved exactly. It is shown that the natural frequency of symmetric angle-ply are generally higher than their antisymmetric counterpart. Also the results are in good agreement with similar results found in literatures.

**Key words:** elasticity solution; laminated; orthotropic; free vibrations; dynamic loading; cylindrical shell.

---

## 1. Introduction

Shell structures are usually analyzed by employing approximate two-dimensional theories based on either the classical Kirchhoff-Love hypothesis of nondeformable normals, (CST) or refinements to it to include the effect of transverse shear deformation and normal stretch. However, to assess the validity of these approximate theories, rigorous solutions based on the three-dimensional theory of elasticity should be obtained for some shell problems which are amenable to such analysis. Such benchmark elasticity solutions are very valuable, especially for laminated composite structures, wherein the inherent anisotropy and inhomogeneity lead to considerable warping of the normal to the middle surface of the shell, and to abrupt variations of the stress at the interfaces of the laminate (Bhaskar, Vardan 1993). Coupled with this,

---

† Associate Professor

‡ Professor

†† Assistant Professor

there has been a growing interest in three-dimensional solutions for laminates, and a number of simple test cases have been analyzed, using the elasticity approach. Although such benchmark results for laminated composite plates have been available for about two decades now (Pagano 1969, 1972), three-dimensional solutions of laminated fiber-reinforced shells are of more recent origin (Chanrashekhara and Kumar 1993, Zhou and Yang 1995).

A simple solution have been presented for cross-ply laminated shell subjected to axisymmetric loading, by assuming that the ratio of thickness to radius is small, and hence can be neglected with respect to unity (Li and Wang 1986). This assumption makes it possible to convert governing differential equations with variable coefficients to the ones with constant coefficients.

Based on the aforementioned approximate elasticity approach, the free vibration problem for homogeneous, isotropic closed cylinders and open panels of finite length with simply supported boundary conditions was obtained (Soldatos and Hadjigeorgiou 1990). Extensive work was done on the torsional vibrations of orthotropic closed cylinders and good agreement between approximate results and exact elasticity solution was observed (Soldatos 1991). A similar approach has been used to study the dynamic response of a doubly curved laminated shell (Bhimaraddi 1991). Using the complete equations of elasticity, the weak form of the equations of motion for laminated anisotropic cylindrical shells were solved, using the Ritz method (Heyliger and Jilani 1993). A solution for the axisymmetric vibration problems of cross-ply laminated closed cylinder was also obtained (Hawkes and Soldatos 1992). The solution of the problem is achieved, using a method of successive approximation. A set of linear three-dimensional frequency equations that describes the vibratory characteristics of elastic solid cylinders of different supports was derived. From the displacement-based energy expression, the variational form of the three-dimensional energy functional was minimized to yield the linear eigenvalue equation. Frequency solutions for elastic solid cylinders of different length and end support conditions were determined (Liew and Hung 1995).

Recently the laminated orthotropic cylindrical shell under blast and patch loads, using elasticity approach have been considered (Shakeri and Yas 1996). The solution is achieved by analytical and finite element solutions. Also three-dimensional axisymmetric vibrations of orthotropic and cross-ply laminated hemispherical shells have been studied (Shakeri and Yas 1995). The solution is obtained by using power series and successive approximation method.

In this paper three-dimensional dynamic response of axisymmetric arbitrary laminated cylindrical shells of finite lengths are studied, and the results are compared with other suitable results found in the literatures.

## **2. The problem formulation**

Consider a laminated composite cylinder made of  $M$  perfectly bonded homogeneous anisotropic layers whose principal axes coincide with three orthogonal coordinates,  $r$ ,  $\theta$  and  $x$  as shown in Fig. 1. The  $r$ ,  $\theta$  and  $x$  represent the radial, circumferential and axial coordinates respectively. Each layer of composite has one plane of elastic symmetry perpendicular to the thickness direction. The material axes of any layer are not necessarily aligned with the  $\theta$  and  $x$  directions, so that the shell conforms to what is generally designated as a laminated anisotropic shell. The constitutive equations of each layer in which 13 elastic constants are involved are stated as

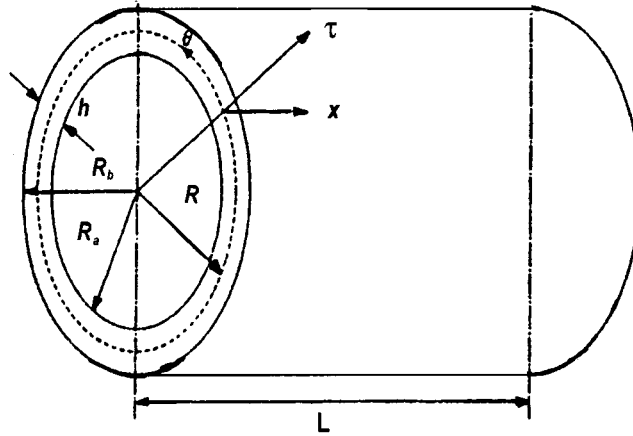


Fig. 1 Coordinates system and geometry of cylindrical shells

$$\begin{bmatrix} \sigma_x \\ \sigma_\theta \\ \sigma_r \\ \tau_{r\theta} \\ \tau_{xr} \\ \tau_{x\theta} \end{bmatrix} = \begin{bmatrix} C_{11} & C_{12} & C_{13} & 0 & 0 & C_{16} \\ C_{12} & C_{22} & C_{23} & 0 & 0 & C_{26} \\ C_{13} & C_{23} & C_{33} & 0 & 0 & C_{36} \\ 0 & 0 & 0 & C_{44} & C_{45} & 0 \\ 0 & 0 & 0 & C_{45} & C_{55} & 0 \\ C_{16} & C_{26} & C_{36} & 0 & 0 & C_{66} \end{bmatrix} \begin{bmatrix} \varepsilon_x \\ \varepsilon_\theta \\ \varepsilon_r \\ \gamma_{r\theta} \\ \gamma_{xr} \\ \gamma_{x\theta} \end{bmatrix} \quad (1)$$

The governing equations of three-dimensional boundary value problem are as follows

$$\begin{aligned} \frac{\partial \sigma_x}{\partial x} + \frac{\partial \tau_{x\theta}}{r \partial \theta} + \frac{\partial \tau_{rx}}{\partial r} + \frac{\tau_{rx}}{r} &= \rho \frac{\partial^2 u_x}{\partial t^2} \\ \frac{\partial \tau_{\theta x}}{\partial x} + \frac{\partial \sigma_\theta}{r \partial \theta} + \frac{\partial \tau_{r\theta}}{\partial r} + \frac{2\tau_{r\theta}}{r} &= \rho \frac{\partial^2 u_\theta}{\partial t^2} \\ \frac{\partial \tau_{xr}}{\partial x} + \frac{\partial \tau_{\theta r}}{r \partial \theta} + \frac{\partial \sigma_r}{\partial r} + \frac{\sigma_r - \sigma_\theta}{r} &= \rho \frac{\partial^2 u_r}{\partial t^2} \end{aligned} \quad (2)$$

Strain-displacement relations are expressed as

$$\begin{aligned} \varepsilon_r &= \frac{\partial u_r}{\partial r} & \varepsilon_\theta &= \frac{u_r}{r} + \frac{\partial u_\theta}{r \partial \theta} & \varepsilon_x &= \frac{\partial u_x}{\partial x} \\ \gamma_{r\theta} &= -\frac{u_\theta}{r} + \frac{\partial u_\theta}{\partial r} + \frac{\partial u_r}{r \partial \theta} & \gamma_{xr} &= \frac{\partial u_x}{\partial r} + \frac{\partial u_r}{\partial x} & \gamma_{x\theta} &= \frac{\partial u_\theta}{\partial x} + \frac{\partial u_x}{r \partial \theta} \end{aligned} \quad (3)$$

Substituting Eqs. (1) and (3) into Eq. (2), the governing equations in terms of displacement for each layer of cylindrical shell under axisymmetric load become

$$\begin{aligned} C_{33}^k \frac{\partial^2 u_r}{\partial r^2} + C_{33}^k \frac{\partial u_r}{r \partial r} + C_{55}^k \frac{\partial^2 u_r}{\partial x^2} - C_{22}^k \frac{u_r}{r^2} + (C_{36}^k - C_{45}^k - C_{26}^k) \frac{\partial u_\theta}{r \partial x} \\ + (C_{36}^k + C_{45}^k) \frac{\partial^2 u_\theta}{\partial r \partial x} + (C_{13}^k - C_{12}^k) \frac{\partial u_x}{r \partial x} + (C_{13}^k + C_{55}^k) \frac{\partial^2 u_x}{\partial x \partial r} = \rho^k \frac{\partial^2 u_r}{\partial t^2} \end{aligned}$$

$$\begin{aligned}
& (2C_{45}^k + C_{26}^k) \frac{\partial u_r}{r \partial x} + (C_{45}^k + C_{36}^k) \frac{\partial^2 u_r}{\partial x \partial r} + C_{44}^k \frac{\partial^2 u_\theta}{\partial r^2} + C_{44}^k \frac{\partial u_\theta}{r \partial r} - C_{44}^k \frac{u_\theta}{r^2} \\
& + C_{66}^k \frac{\partial^2 u_\theta}{\partial x^2} + C_{45}^k \frac{\partial^2 u_x}{\partial r^2} + 2C_{45}^k \frac{\partial u_x}{r \partial r} + C_{16}^k \frac{\partial^2 u_x}{\partial x^2} = \rho^k \frac{\partial^2 u_\theta}{\partial t^2} \\
& (C_{12}^k + C_{55}^k) \frac{\partial u_r}{r \partial x} + (C_{13}^k + C_{55}^k) \frac{\partial^2 u_r}{\partial x \partial r} + C_{45}^k \frac{\partial^2 u_\theta}{\partial r^2} + C_{16}^k \frac{\partial^2 u_\theta}{\partial x^2} + C_{11}^k \frac{\partial^2 u_n}{\partial n^2} \\
& + C_{55}^k \left( \frac{\partial^2 u_x}{\partial r^2} + \frac{\partial u_x}{r \partial r} \right) = \rho^k \frac{\partial^2 u_x}{\partial t^2}
\end{aligned} \tag{4}$$

The simply supported boundary conditions are taken as

$$\sigma_x = u_r = 0 \quad \text{at} \quad x = 0, L \tag{5}$$

For a laminate consisting of  $M$  laminas, the continuity conditions to be enforced at any arbitrary interior  $k$ th interface can be written as

$$\begin{aligned}
(\sigma_r)_k &= (\sigma_r)_{k+1} & (\tau_{xr})_k &= (\tau_{xr})_{k+1} & (\tau_{\theta r})_k &= (\tau_{\theta r})_{k+1} \\
(u_r)_k &= (u_r)_{k+1} & (u_\theta)_k &= (u_\theta)_{k+1} & (u_x)_k &= (u_x)_{k+1}
\end{aligned}$$

where the suffix  $k$  and  $k+1$  represents the corresponding stresses and displacements at the  $k$ th and  $(k+1)$ th laminas. The above formulations are used to analyse a multilayered cylindrical shell as well as the free vibrations of the shell.

### 3. Part I-Deformation and stress analysis of the shell

The solution which satisfies the boundary conditions (5) can be taken as

$$\begin{aligned}
u_r &= \sum_{m=1}^{\infty} \sin(P_m x) u_r(r, t) \\
u_\theta &= \sum_{m=1}^{\infty} \cos(P_m x) u_\theta(r, t) \\
u_x &= \sum_{m=1}^{\infty} \cos(P_m x) u_x(r, t) \quad \text{where} \quad P_m = \frac{m\pi}{L}
\end{aligned} \tag{7}$$

The boundary conditions on the inner and outer surfaces of the shell are taken as

$$\begin{aligned}
\sigma_r = F(x, t) \quad \tau_{xr} = \tau_{r\theta} = 0 & \quad \text{At the inner surface} \\
\sigma_r = \tau_{xr} = \tau_{r\theta} = 0 & \quad \text{At the outer surface}
\end{aligned} \tag{8}$$

The dynamic load is uniform along the axial direction and is presented by a Fourier series with respect to the  $x$  axis as

$$F(x, t) = \sum_{m=1}^{\infty} \left[ \frac{4}{\pi m} \sin(P_m x) \right] F(t) \tag{9}$$

Substituting Eqs. (7) into (4) yields

$$C_{33}^k \frac{\partial u_r^2}{\partial r^2} + C_{33}^k \frac{\partial u_r}{r \partial r} - C_{55}^k P_m^2 u_r - C_{22}^k \frac{u_r}{r^2} - (C_{36}^k - C_{45}^k - C_{26}^k) P_m \frac{u_\theta}{r}$$

$$\begin{aligned}
 &-(C_{36}^k + C_{45}^k)P_m \frac{\partial u_\theta}{\partial r} - (C_{13}^k - C_{12}^k)P_m \frac{u_x}{r} - (C_{13}^k + C_{55}^k)P_m \frac{\partial u_x}{\partial r} = \rho^k \frac{\partial^2 u_r}{\partial t^2} \\
 &(2C_{45}^k + C_{26}^k)P_m \frac{u_r}{r} + (C_{45}^k + C_{36}^k)P_m \frac{\partial u_r}{\partial r} + C_{44}^k \frac{\partial^2 u_\theta}{\partial r^2} + C_{44}^k \frac{\partial u_\theta}{r \partial r} - C_{44}^k \frac{u_\theta}{r^2} \\
 &\quad - C_{66}^k P_m^2 u_\theta + C_{45}^k \frac{\partial^2 u_x}{\partial r^2} + 2C_{45}^k \frac{\partial u_x}{r \partial r} - C_{16}^k P_m^2 u_x = \rho^k \frac{\partial^2 u_\theta}{\partial t^2} \\
 &(C_{12}^k + C_{55}^k)P_m \frac{u_r}{r} + (C_{13}^k + C_{55}^k)P_m \frac{\partial u_r}{\partial r} + C_{45}^k \frac{\partial^2 u_\theta}{\partial r^2} - C_{16}^k P_m^2 u_\theta - C_{11}^k P_m^2 u_x \\
 &\quad + C_{55}^k \left( \frac{\partial^2 u_x}{\partial r^2} + \frac{\partial u_x}{r \partial r} \right) = \rho^k \frac{\partial^2 u_x}{\partial t^2} \tag{10}
 \end{aligned}$$

The Galerkin method is used to obtain the finite element model of shell. A Kantorovich type of approximation for space and time domains is employed and the space domain is approximated by linear shape functions. Selection of linear shape functions is based on the prior experience of the authors with Galerkin method (Eslami, Alizadeh 1990, Eslami, Shakeri, Yas 1994).

Considering linear shape functions for the three field variables  $u_r$ ,  $u_\theta$  and  $u_x$  as

$$\begin{aligned}
 u_r &= \langle N_1 \rangle \{U_r\} \\
 u_\theta &= \langle N_1 \rangle \{U_\theta\} \\
 u_x &= \langle N_1 \rangle \{U_x\} \tag{11}
 \end{aligned}$$

and applying the formal Galerkin method to the governing Eqs. (10), results into the following dynamic finite element equilibrium equation for each layer

$$[M]_k \{\ddot{X}\} + [K]_k \{X\} = \{0\} \tag{12}$$

The elements of mass and stiffness matrices are given in appendix A. For nodes which are located at any arbitrary interior  $k$ th and  $(k+1)$ th interfaces as Fig. 2, the continuity are written as

$$\begin{aligned}
 U_{rkl}^k &= U_{rkl+1}^{k+1} & \sigma_{rkl}^k &= \sigma_{rkl+1}^{k+1} \\
 U_{\theta kl}^k &= U_{\theta kl+1}^{k+1} & \tau_{r\theta kl}^k &= \tau_{r\theta kl+1}^{k+1} \\
 U_{xkl}^k &= U_{xkl+1}^{k+1} & \tau_{xrkl}^k &= \tau_{xrkl+1}^{k+1} \tag{13}
 \end{aligned}$$

Deriving Eqs. (13) in terms of displacements and expressing the derivatives in backward and forward finite difference for  $k$ th and  $(k+1)$ th layers respectively, one can obtain

$$\begin{aligned}
 &C_{13}^k (-P_m U_{xkl}^k) + C_{23}^k \frac{U_{rkl}^k}{R_k} + C_{23}^k \frac{U_{rkl}^k - U_{rkl-1}^k}{h_e} - C_{36}^k P_m U_{\theta kl}^k = C_{13}^{k+1} (-P_m U_{xkl+1}^{k+1}) \\
 &\quad + C_{23}^{k+1} \frac{U_{rkl+1}^{k+1}}{R_{k+1}} + C_{23}^{k+1} \frac{U_{rkl+2}^{k+1} - U_{rkl+1}^{k+1}}{h_e} - C_{36}^{k+1} P_m U_{\theta kl+1}^{k+1} \\
 &C_{44}^{k+1} \left( -\frac{U_{\theta kl}^k}{R_k} + \frac{U_{\theta kl}^k - U_{\theta kl-1}^k}{h_e} \right) + C_{44}^k \left( \frac{U_{xkl}^k - U_{xkl-1}^k}{h_e} + P_m U_{rkl}^k \right)
 \end{aligned}$$

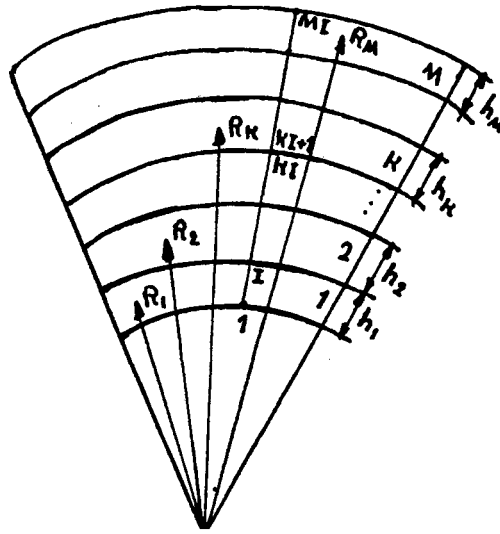


Fig. 2 Nomenclature of a subdivided cylinder

$$\begin{aligned}
 &= C_{44}^{k+1} \left( -\frac{U_{\theta kl+1}^{k+1}}{R_{k+1}} + \frac{U_{\theta kl+2}^{k+1} - U_{\theta kl+1}^{k+1}}{h_e} \right) + C_{44}^{k+1} \left( \frac{U_{xkl+2}^{k+1} - U_{xkl+1}^{k+1}}{h_e} + P_m U_{rkl+1}^{k+1} \right) \\
 &\quad C_{45}^k \left( \frac{U_{\theta kl}^k}{R_k} + \frac{U_{\theta kl}^k - U_{\theta kl-1}^k}{h_e} \right) + C_{55}^k \left( \frac{U_{xkl}^k - U_{xkl-1}^k}{h_e} + P_m U_{rkl}^k \right) \\
 &= C_{45}^{k+1} \left( -\frac{U_{\theta kl+1}^{k+1}}{R_{k+1}} + \frac{U_{\theta kl+2}^{k+1} - U_{\theta kl+1}^{k+1}}{h_e} \right) + C_{55}^{k+1} \left( \frac{U_{xkl+2}^{k+1} - U_{xkl+1}^{k+1}}{h_e} + P_m U_{rkl+1}^{k+1} \right) \tag{14}
 \end{aligned}$$

$U_{rkl}$ ,  $U_{\theta kl}$  and  $U_{xkl}$  are obtained from the above algebraic equations in terms of displacement values of neighbouring nodes as

$$\begin{aligned}
 U_{rkl}^k &= U_{rkl+1}^{k+1} = AU_{rkl-1}^k + BU_{rkl+2}^{k+1} + CU_{\theta kl-1}^k + DU_{\theta kl+2}^{k+1} + EU_{xkl-1}^k + FU_{xkl+2}^{k+1} \\
 U_{\theta kl}^k &= U_{\theta kl+1}^{k+1} = A'U_{rkl-1}^k + B'U_{rkl+2}^{k+1} + C'U_{\theta kl-1}^k + D'U_{\theta kl+2}^{k+1} + E'U_{xkl-1}^k + F'U_{xkl+2}^{k+1} \\
 U_{xkl}^k &= U_{xkl+1}^{k+1} = A''U_{rkl-1}^k + B''U_{rkl+2}^{k+1} + C''U_{\theta kl-1}^k + D''U_{\theta kl+2}^{k+1} + E''U_{xkl-1}^k + F''U_{xkl+2}^{k+1} \tag{15}
 \end{aligned}$$

The coefficients of  $A \dots A', \dots A'' \dots F$  are constant and are given in Appendix.

The dynamic finite element equilibrium equations for two neighbouring at interior  $k$ th and  $(k+1)$ th interfaces become

$$[M]_k \{\ddot{X}\}_k + [K]_k \{X\}_k = \{0\} \tag{16a}$$

$$[M]_{k+1} \{\ddot{X}\}_{k+1} + [K]_{k+1} \{X\}_{k+1} = \{0\} \tag{16b}$$

where  $\{x\}_k^T = \{x\}_{k+1}^T = \{U_{rkl-1}, U_{rkl+2}, U_{\theta kl-1}, U_{\theta kl+2}, U_{xkl-1}, U_{xkl+2}\}$ . The elements of mass and stiffness matrices are also given in Appendix.

Applying traction conditions (8) and expressing the derivatives in backward and forward finite differences for last and first elements respectively, a system of algebraic equations are obtained

$$\begin{aligned}
 & C_{13}^M (-P_m U_{xMI}^M) + C_{23}^M \frac{U_{rMI}^M}{R_b} + C_{23}^M \frac{U_{rMI}^M - U_{rMI-1}^M}{h_e} - C_{36}^M P_m U_{\theta MI}^M = 0 \\
 & C_{44}^M \left( -\frac{U_{\theta MI}^M}{R_b} + \frac{U_{\theta MI}^M - U_{\theta MI-1}^M}{h_e} \right) + C_{45}^M \left( \frac{U_{xMI}^M - U_{xMI-1}^M}{h_e} + P_m U_{rMI}^M \right) = 0 \\
 & C_{45}^M \left( -\frac{U_{\theta MI}^M}{R_b} + \frac{U_{\theta MI}^M - U_{\theta MI-1}^M}{h_e} \right) + C_{55}^M \left( \frac{U_{xMI}^M - U_{xMI-1}^M}{h_e} + P_m U_{rMI}^M \right) = 0 \\
 & C_{13}^1 (-P_m U_{x1}) + C_{23}^1 \frac{U_{r1}}{R_a} + C_{23}^1 \frac{U_{r2} - U_{r1}}{h_e} - C_{36}^1 P_m U_{\theta 1} = F(t) \\
 & C_{44}^1 \left( -\frac{U_{\theta 1}}{R_a} + \frac{U_{\theta 2} - U_{\theta 1}}{h_e} \right) + C_{45}^1 \left( \frac{U_{x2} - U_{x1}}{h_e} + P_m U_{r1} \right) = 0 \\
 & C_{45}^1 \left( -\frac{U_{\theta 1}}{R_a} + \frac{U_{\theta 2} - U_{\theta 1}}{h_e} \right) + C_{55}^1 \left( \frac{U_{x2} - U_{x1}}{h_e} + P_m U_{r1} \right) = 0 \tag{17}
 \end{aligned}$$

From the above algebraic equations  $U_{rMI}$ ,  $U_{\theta MI}$ ,  $U_{xMI}$ ,  $U_{r1}$ ,  $U_{\theta 1}$ ,  $U_{x1}$  are obtained in terms of the neighbouring nodes values. Therefore the dynamic equilibrium equations for the last and first elements become

$$[M]_{MI-1} \{\ddot{X}\}_{MI-1} + [K]_{MI-1} \{X\}_{MI-1} = \{0\} \tag{18a}$$

$$[M]_1 \{\ddot{X}\}_1 + [K]_1 \{X\}_1 = \{F(t)\} \tag{18b}$$

$$\text{where } \{x\}_1^T = \{U_{r2}, U_{\theta 2}, U_{x2}\} \quad \{x\}_{MI-1}^T = \{U_{rMI-1}, U_{\theta MI-1}, U_{xMI-1}\}$$

By assembling Eqs. (12), (16a, b) and (18a, b) the general dynamic finite element equilibrium equations are obtained.

Once the finite element equilibrium equation is established, different numerical method can be employed to solve them in space and time domains. The Newmark direct integration method with suitable time step is used and the equilibrium equation is solved.

#### 4. Part II-Free vibrations analysis of shell

To study the free vibration of the shell, the inner and outer surfaces are taken to be traction free. Thus

$$\sigma_r = \tau_{r\theta} = \tau_{\theta r} = 0 \tag{19}$$

The coefficients of the Eq. (4) are functions of variable  $r$  which makes the solution formidable. To circumvent this difficulty, we make use of the following change of variable (Jing and Tzeng 1993)

$$\frac{1}{r} = \frac{1}{R_k} (1 - \eta_k) \quad \frac{1}{r^2} = \frac{1}{R_k^2} (1 - 2\eta_k)$$

where

$$\eta_k = \frac{r}{R_k} - 1 \quad |\eta_k| \ll 1$$

Eq. (4) in terms of the new variable become

$$\begin{aligned} & C_{33}^k \frac{\partial u_r^2}{\partial \eta_k^2} + C_{33}^k \frac{\partial u_r}{\partial \eta_k} + C_{55}^k R_k^2 \frac{\partial^2 u_r}{\partial x^2} - C_{22}^k u_r + R_k \left[ (C_{36}^k - C_{45}^k - C_{26}^k) \frac{\partial u_\theta}{\partial x} \right. \\ & \left. + (C_{36}^k + C_{45}^k) \frac{\partial^2 u_\theta}{\partial x \partial \eta_k} \right] + (C_{13}^k - C_{12}^k) \frac{\partial u_x}{\partial x} + (C_{13}^k + C_{55}^k) \frac{\partial^2 u_x}{\partial \eta_k \partial x} = \rho^k R_k^2 \frac{\partial^2 u_r}{\partial t^2} \\ & R_k \left[ (2C_{45}^k + C_{26}^k) \frac{\partial u_r}{\partial x} + (C_{45}^k + C_{36}^k) \frac{\partial^2 u_r}{\partial x \partial \eta_k} \right] + C_{44}^k \frac{\partial^2 u_\theta}{\partial \eta_k^2} + C_{44}^k \frac{\partial u_\theta}{\partial \eta_k} - C_{44}^k u_\theta \\ & + C_{66}^k R_k^2 \frac{\partial^2 u_\theta}{\partial x^2} + C_{45}^k \frac{\partial^2 u_x}{\partial \eta_k^2} + 2C_{45}^k \frac{\partial u_x}{\partial \eta_k} + C_{16}^k R_k^2 \frac{\partial^2 u_x}{\partial x^2} = \rho^k R_k^2 \frac{\partial^2 u_\theta}{\partial t^2} \\ & R_k \left[ (C_{12}^k + C_{55}^k) \frac{\partial u_r}{\partial x} + (C_{13}^k + C_{55}^k) \frac{\partial^2 u_r}{\partial x \partial \eta_k} \right] + C_{45}^k \frac{\partial^2 u_\theta}{\partial \eta_k^2} + C_{16}^k R_k^2 \frac{\partial^2 u_\theta}{\partial x^2} \\ & + C_{11}^k R_k^2 \frac{\partial^2 u_x}{\partial x^2} + C_{55}^k \left( \frac{\partial^2 u_x}{\partial \eta_k^2} + \frac{\partial u_x}{\partial \eta_k} \right) = \rho^k R_k^2 \frac{\partial^2 u_x}{\partial t^2} \end{aligned} \tag{20}$$

The solution to Eq. (20) which identically satisfies the boundary conditions on the two ends are considered as

$$\begin{aligned} u_r^k(x, \eta, t) &= \sum_m \sin P_m x A_r(\eta) e^{i\alpha t} \\ u_\theta^k(x, \eta, t) &= \sum_m \cos P_m x A_\theta(\eta) e^{i\alpha t} \\ u_x^k(x, \eta, t) &= \sum_m \cos P_m x A_x(\eta) e^{i\alpha t} \end{aligned} \tag{21}$$

The substitution of Eq. (21) into (20) yields a system of homogeneous ordinary differential equations, which the solution to those are

$$\begin{aligned} A_r(\eta_k) &= u_r^* e^{\lambda \eta} \\ A_\theta(\eta_k) &= u_\theta^* e^{\lambda \eta} \\ A_x(\eta_k) &= u_x^* e^{\lambda \eta} \end{aligned} \tag{22}$$

Where  $u_r^*$ ,  $u_\theta^*$  and  $u_x^*$  are the unknown coefficients. Upon inserting solutions (22), we arrive at a system of homogeneous algebraic equations, which may be written in matrix form as

$$[A] \{U\} = \{0\}$$

where

$$\{U\}^T = \{u_r^*, u_\theta^*, u_x^*\} \tag{23}$$

The conditions of Eq. (23) to have nontrivial solution is that the determinate of matrix A should vanish. This leads to the sixth following order algebraic equation



$$A \lambda^6 + B \lambda^5 + C \lambda^4 + D \lambda^3 + E \lambda^2 + F \lambda + G = 0 \tag{24}$$

The displacement components may be obtained which are functions of natural frequency  $\omega$ . Substituting the roots of Eq. (24) into (21) yields

$$\begin{aligned} u^k(x, \eta, t) &= \sum_m \sum_{j=1}^6 K_{mj}^k e^{\lambda_j \eta} \sin P_m x e^{i \alpha t} \\ u^{\delta}(x, \eta, t) &= \sum_m \sum_{j=1}^6 P_{mj}^k K_{mj}^k e^{\lambda_j \eta} \cos P_m x e^{i \alpha t} \\ u^k(x, \eta, t) &= \sum_m \sum_{j=1}^6 Q_{mj}^k K_{mj}^k e^{\lambda_j \eta} \cos P_m x e^{i \alpha t} \end{aligned} \tag{25}$$

where  $P_{mj}^k$  and  $Q_{mj}^k$  are function of  $\omega$ . Substituting (25) into the traction free condition (19) and continuity requirements (6) leads to a system of  $6M$  homogeneous algebraic equations, which can be represented in the following matrix form

$$[H]\{K\} = \{0\} \tag{26}$$

The vector  $\{K\}$  is the mode shape. The component of  $[H]$  which is a  $6M * 6M$  matrix are function of natural frequency. From Eq. (26) we have

$$|H| = 0 \tag{27}$$

Eqs. (27) and (24) should be solved simultaneously by the successive approximation procedure to obtain the first few natural frequencies of the shell.

### 5. Numerical results and discussion

As a first example cylindrical shells of graphite/epoxy materials are analyzed under dynamic loads. For this purpose closed cylindrical shells composed of two unsymmetric layers [45/0] and symmetric angle-ply layer [45/-45/45] are studied. The loading configuration is shown in Fig. 3.

The loading equation can be expressed as

$$F(x, t) = \sum_m F_o (1 - e^{-13100t}) \sin P_m x$$

The positive sign of the fiber denote counterclockwise direction with respect to the positive

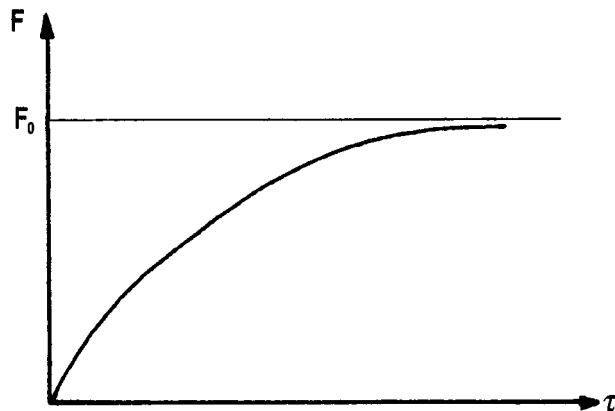


Fig. 3 Dynamic load

Table 1 Effect of  $\Delta t$  for a [45/0] angle-ply

$\Delta t$	$\bar{u}_r$	$\bar{\sigma}_\theta$	$\bar{\sigma}_x$
1.5E-3	5.2841	1.9832	-1.1347
6E-4	6.0377	2.3495	-1.1873
3E-4	6.2502	2.6274	-1.3701
1E-4	6.2530	2.6311	-1.3763

All the values are given at the middle of length and  $t=0.5$  Msec,  $N=200$ .

Table 2 Effect of number of elements for a [45/0] angle-ply

$N$	$\bar{u}_r$	$\bar{\sigma}_\theta$	$\bar{\sigma}_x$
25	5.1912	1.8312	-1.1294
50	5.9305	2.3015	-1.1763
100	6.2473	2.6269	-1.3699
200	6.2530	2.6311	-1.3763

All the values are given at the middle of length and  $t=0.5$  Msec,  $\Delta t=1E-4$ .

direction of the  $x$  axis. Material properties and nondimensionalized deformations and stresses are considered as follows

$$\frac{E_L}{E_T} = 40 \quad \frac{G_{LT}}{E_T} = 0.5 \quad \frac{G_{TT}}{E_T} = 0.2 \quad \nu_{LT} = 0.25 \quad \nu_{TT} = 0.49$$

$$\frac{R}{h} = 5 \quad \frac{L}{R} = 20$$

$$(\bar{u}_r, \bar{u}_\theta, \bar{u}_x) = \frac{E_T h}{F_o R^2} (10u_r, 20u_\theta, u_x)$$

$$(\bar{\sigma}_r, \bar{\sigma}_\theta, \bar{\sigma}_x, \bar{\tau}_{r\theta}, \bar{\tau}_{xr}, \bar{\tau}_{x\theta}) = \frac{1}{F_o} (\sigma_r, \sigma_\theta, \sigma_x, \tau_{r\theta}, \tau_{xr}, \tau_{x\theta})$$

The layers are of equal thickness. As a first step, the efficiency of the method is studied. For this purpose in Table 1 and 2 effect of time increment  $\Delta t$  and the number of elements on the results and computational times are shown. In Table 1 four different  $\Delta t$  from 1.5E-3 up to 1E-4 and in Table 2 four different element number (25, 50, 100, 200) are considered. It is noticed that  $\Delta t=1E-4$  and  $N=200$  are suitable for computation and with respect to these values, the calculation require less time.

The radial displacement history at  $r=R$  for the middle length of the shell is shown in Fig. 4 and is compared with HSD results (Eslami, Shakeri, Yas, Barzekar under review) for both stacking sequences, unsymmetric [45/0] and symmetric [45/-45/45]. As it is observed the radial displacement of symmetric angle-ply is generally lower than its unsymmetric counterpart. That is due to the effect of bending-stretching coupling that characterize symmetric laminate. It is also seen that for symmetric angle-ply the difference between ES and HSD results become higher. In Figs. 5 to 8 the axial variations of inplane stresses at inner and outer surfaces are shown for [45/-

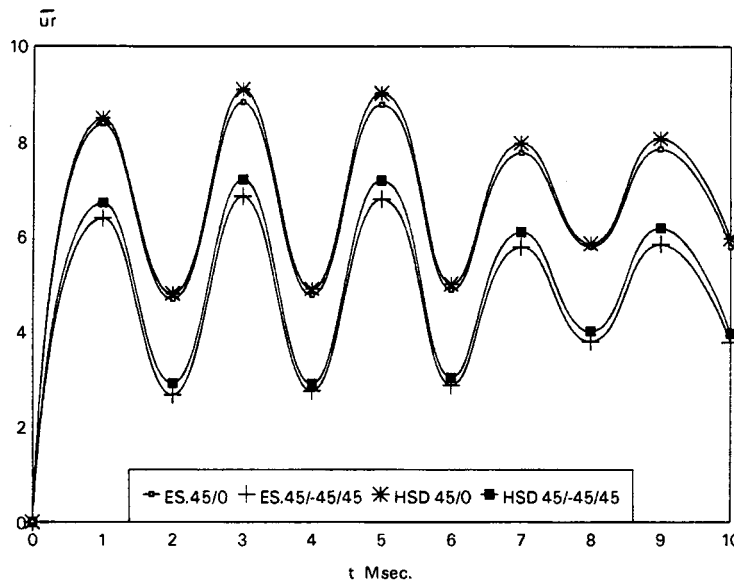


Fig. 4 History of radial displacement

45/45] lamination. The distribution of in-plane stresses along the axial direction is uniform. Some variations can be seen near the edge region due to the edge effects, just as the case of isotropic shells (Eslami, Shakeri, Yas 1994). From these figures it is noticed that CST (classical shell theory) solution shows considerable disagreement when compared with the ES solution. The reason of this difference has been suggested to be due to the initial curvature effect combined with the effect of material properties (Jing and Tzeng 1993). In another word this effect can be

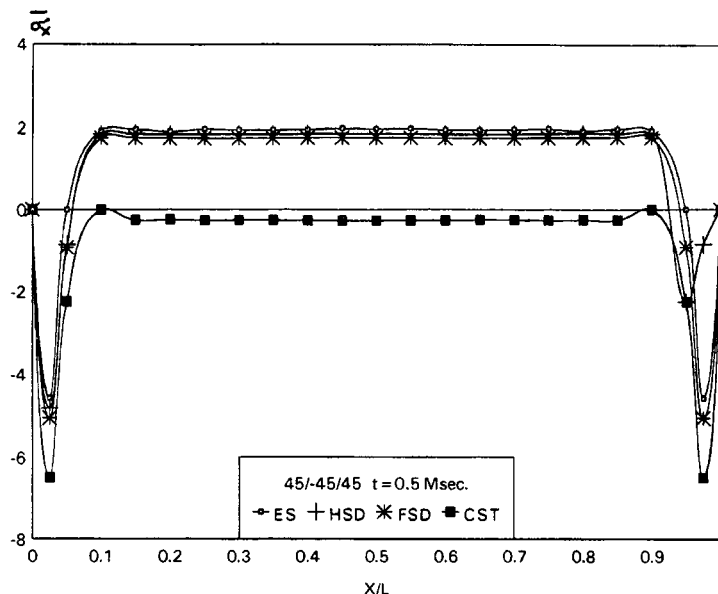


Fig. 5 Axial variation of longitudinal stress on the inner surface

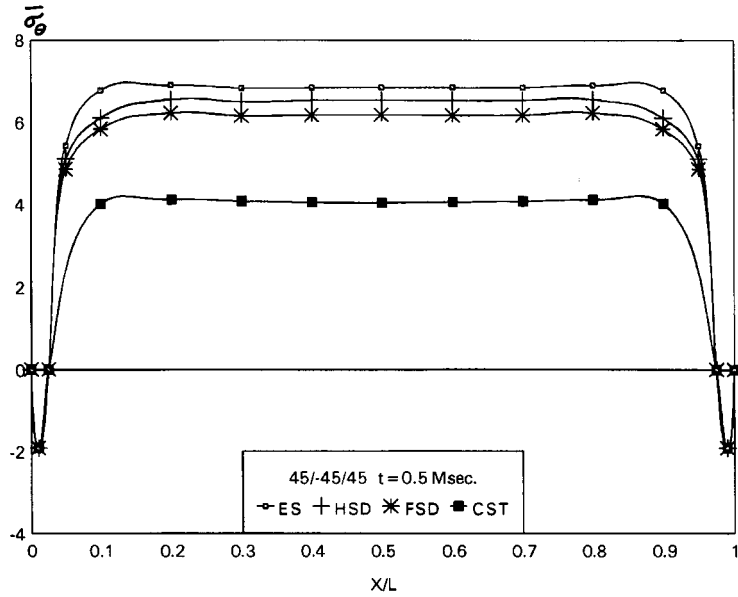


Fig. 6 Axial variation of circumferential stress on the inner surface

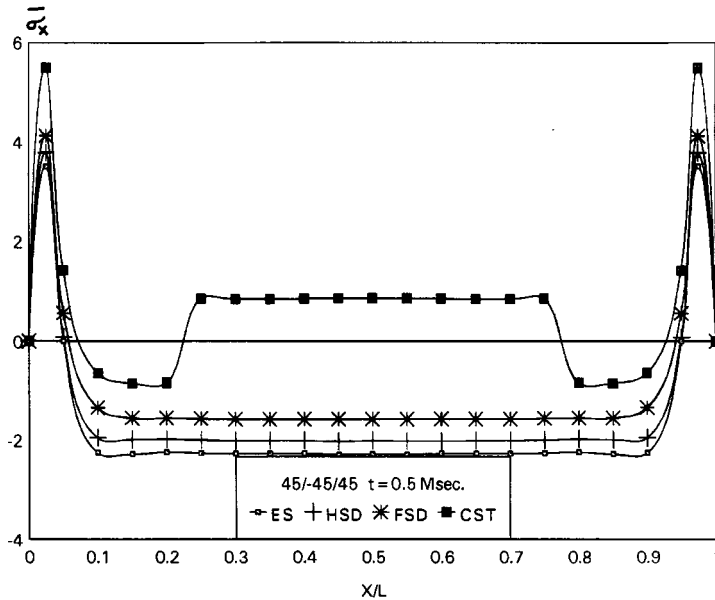


Fig. 7 Axial variation of longitudinal stress on the outer surface

explained in terms of thickness. In calculating  $\bar{\sigma}_x$ ,  $\bar{\sigma}_\theta$ ,  $\bar{\tau}_{x\theta}$ , the hoop strain  $\epsilon_\theta$  is involved as well as the radius of curvature. The radius of curvature is smaller on the inner surface than the mean radius and larger on the outer surface. Furthermore as shown by constitutive equation under this stacking sequence, the corresponding material constant e.g.,  $C_{12}$  for  $\bar{\sigma}_x$  is comparable to the major constant, e.g.,  $C_{11}$ . The influence of  $\epsilon_\theta$  on  $\bar{\sigma}_x$ ,  $\bar{\sigma}_\theta$ , and  $\bar{\tau}_{x\theta}$  is then obvious. The FSD (first order shear deformation theory) fall between those for CST and HSD. Fig. 9 shows the variations of

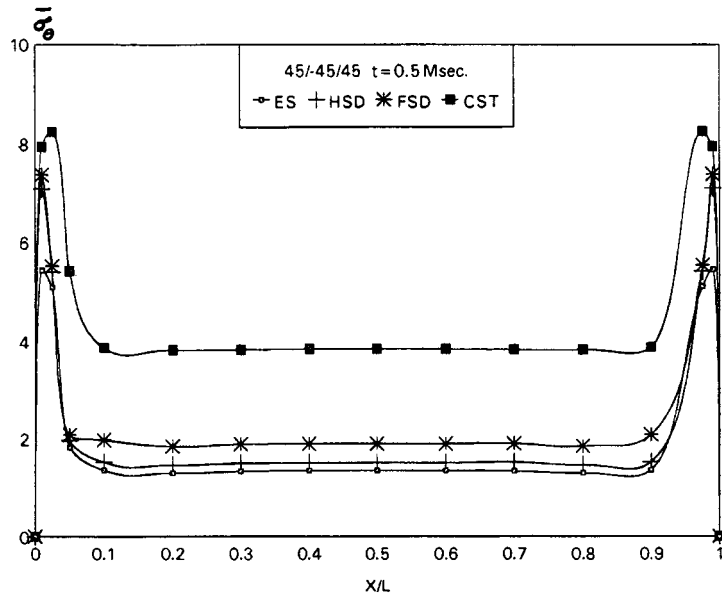


Fig. 8 Axial variation of circumferential stress on the outer surface

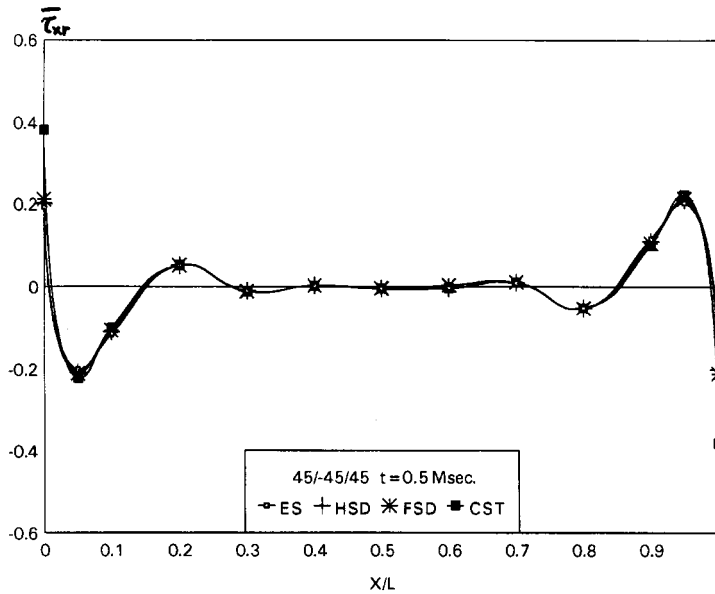


Fig. 9 Axial variation of transverse shear stress ( $\bar{\tau}_{xr}$ ) on the middle surface

transverse shear stress  $\bar{\tau}_{xr}$ . It can be seen that  $\bar{\tau}_{xr}$  is zero on the middle surface in central region, reaching higher values at the edges. In this figure the HSD result is compared with ES solution, and maximum deviation is found to be about 1%. The through-thickness distribution of transverse normal stress of three-layer angle-ply [45/-45/45] which has close relation with delamination failure of composite laminates, is shown for four different time values in Fig. 10. In this figure  $\bar{\sigma}_r$  is compression in the top and then changes to tension on downward. Corresponding behavior has

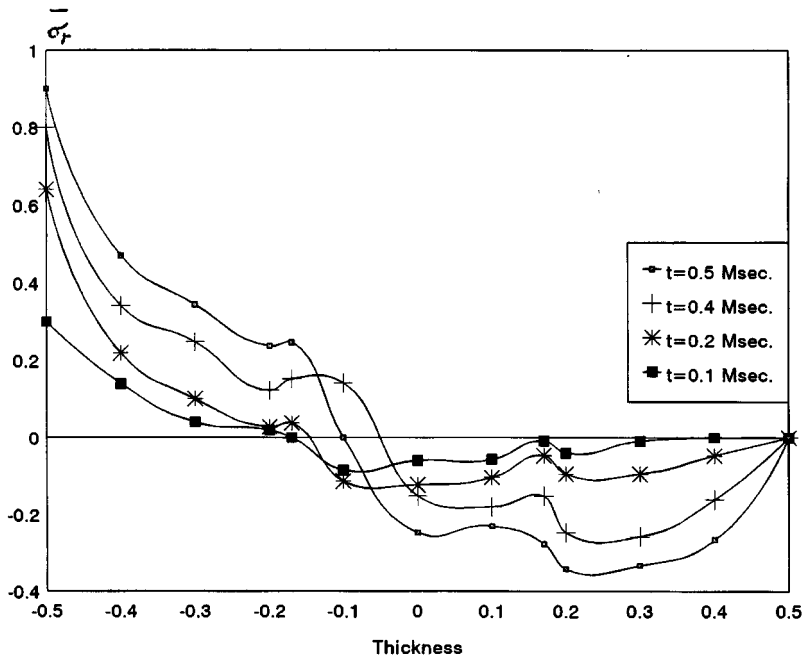


Fig. 10 Through-thickness distribution of transverse normal stress

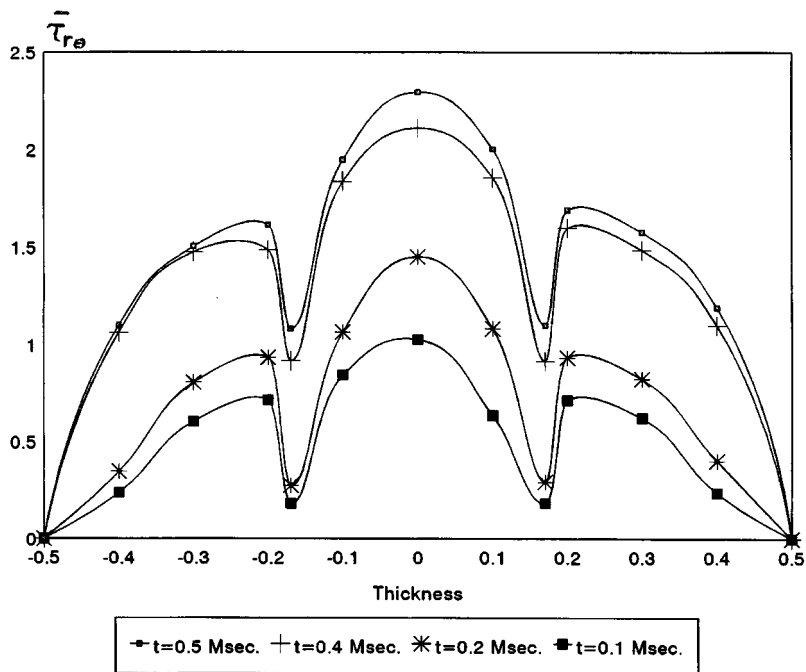


Fig. 11 Through-thickness distribution of transverse shear stress

Table 3 Convergency of the results

$M$	$\bar{\omega}_1$	$\bar{\omega}_2$
2	7.163	8.917
4	7.215	9.014
6	7.362	9.165
8	7.401	9.225
10	7.420	9.233

been reported previously (Ren 1987).

It can be said the change of sign of transverse normal stress is mainly due to the curvature of the shell. It is also noticed that the slope of transverse normal stress is not continuous across the interface. The reason is due to the discontinuity of inplane stresses at the interface as well as the initial curvature.

Fig. 11 shows the variations of transverse shear ( $\bar{\tau}_{r\theta}$ ) with respect to the thickness of the shell for four different time values. Basically the distribution of transverse shear stress in each layer is very close to parabola. Also due to initial curvature, the distribution is not symmetric. Discontinuity of the slope of transverse shear stress across the interface is noticed.

In second example, free vibrations is considered. It is assumed that the layers of laminated cylinder are constructed by graphite/epoxy material, having the following orthotropic properties.

$$\frac{E_L}{E_T} = 15 \quad \frac{G_{LT}}{E_T} = \frac{G_{TT}}{E_T} = 0.428 \quad \nu_{LT} = \nu_{TT} = 0.4$$

The convergence of two first natural frequency parameter,  $\bar{\omega} = \omega L(\rho/E_T)^{0.5}/h$  of two layer [45/0] laminated hollow cylinder is shown in Table 3. The cylinder has middle radius to thickness ratio

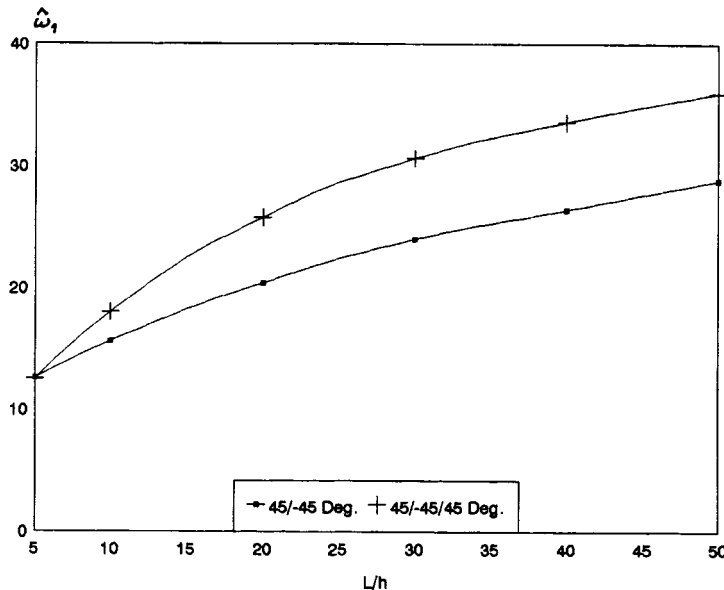


Fig. 12 Variation of first natural frequency parameter

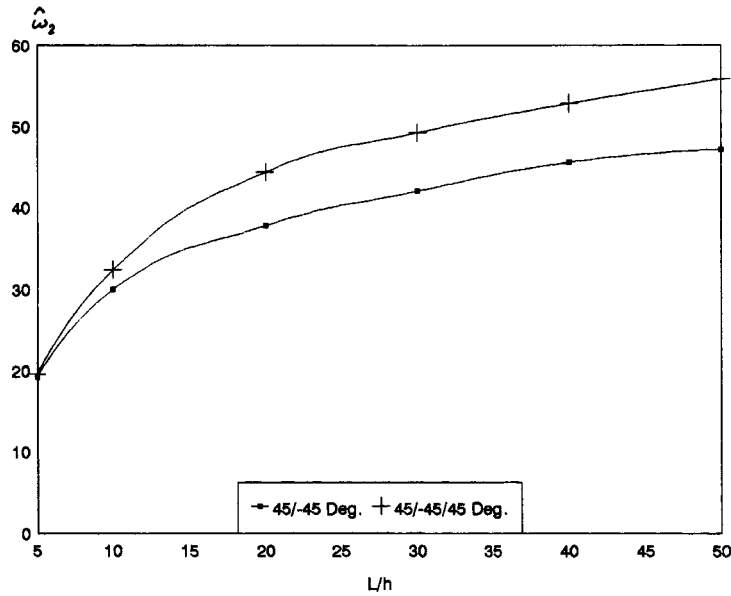


Fig. 13 Variation of second natural frequency parameter

Table 4 Comparison of the lowest

$\frac{R}{h}$	Present	Heyliger
5	2.752	2.797
10	4.511	4.585
20	8.047	8.166
50	19.113	19.464

$R/h=2$  and  $mR/L=1$ . The two layers of cylinder is divided in  $M/2$  mathematical layers. As it is observed, the convergency is fast.

Figs. 12 and 13 exhibit the variation of the two first natural frequency parameter of antisymmetric  $[45/-45]$  and symmetric  $[45/-45/45]$  angle-ply with respect to the length to thickness ratio ( $L/h$ ). The radius to thickness ratio is  $R/h=2$ . As it is noticed the natural frequency of symmetric angle-ply is generally higher than their antisymmetric counterpart in the entire range of  $L/h$  considered and that the corresponding curves have stiffer slopes, especially in the thicker shell regime. This is due to the effect of bending-stretching coupling.

As a check on the accuracy of the computational scheme, two layer cross-ply cylindrical shell composed of graphite/epoxy with the properties

$$E_L = 206.84 \text{ GPa.} \quad E_T = 5.171 \text{ GPa.} \quad \nu_{LT} = 0.25 \quad G_{LT} = 2.585 \text{ GPa.}$$

$$\frac{G_{TT}}{E_T} = 0.416 \quad \frac{R}{h} = 5$$

is considered. The shell in this example has a  $[0/90]$  stacking sequence, which implies that the



fiber in the outer layer run in the circumferential direction and that the fiber in the inner layer run in the axial direction. The results are compared with similar ones found in the literatures based on Ritz method (Heyliger and Jilani 1993) in Table 4. The frequencies are tabulated in terms of the frequency parameter  $\omega^*$  which is defined as

$$\omega^* = \omega \frac{L^2}{\pi^2} \left( \frac{\rho}{D_{11}} \right)^{0.5} \quad \text{where} \quad D_{11} = \frac{1+E_L/E_T}{2} C_{11} \frac{h^3}{12}$$

As it is observed, there is good agreement between the results.

## 6. Conclusions

In this paper three-dimensional layerwise solution of dynamic response of composite cylindrical shell is studied. A Kantorovich type of approximation for space and time domain is approximated by a simple finite element model. The innovation of this model is that the continuity conditions between any two layer, as well as traction conditions are satisfied. The method provides good prediction of dynamic response of composite cylindrical shell, while requiring short computer time. The results show that difference between HSD and ES become higher for symmetric angle-ply due to the effect of bending-stretching coupling. It is found that the general behaviour of laminated shell under dynamic load is similar to that of isotropic shells, e.g., uniform variations of inplane stresses along the axial direction and some variations near the edge regions. It is also concluded that HSD can be used as a good alternative to rigorous three-dimensional analysis. It is observed that due to discontinuity of inplane stresses at the interface and initial curvature, the slope of transverse normal and shear stresses aren't continuous across the interface. Also the through thickness distribution of transverse shear stress in each layer is very close to a parabola and due to initial curvature, this distribution is not symmetric.

For free vibration analysis, the solution is based on the assumption which was made by Li and Wang (Li and Wang 1986). In fact the method of solution is the extension of approach which have been used by Hawkes and Soldatos previously (Hawkes and Soldatos 1992). It is shown that the results are well compared with the similar ones which has been obtained by Heyliger (Heyliger and Jilani 1993), through using Ritz method. In addition the convergenc of the method is fast. The results show that the natural frequency of symmetric angle-ply are generally higher than their antisymmetric counterpart in the entire range of  $L/h$  considered and the corresponding curves have stiffer slopes, especially in the thicker shell regime. In another words for thick shell the difference of natural frequency between symmetric and antisymmetric angle-ply is low, while in the thin shell regime, this difference is considerable.

## References

- Bhaskar, K. and Varadan, T.K. (1993), "Benchmark elasticity solution for locally loaded laminated orthotropic cylindrical shells", *AIAA J.*, **32**, 627-632.
- Bhimaraddi, A. (1991), "Free vibration analysis of doubly curved shallow shells on rectangular planform using three-dimensional elasticity theory", *J. Solids and Structures*, **27**, 897-913.
- Chanrashekhara, K. and Kumar, B.S. (1993), "Static analysis of thick laminated circular cylindrical

- shells”, *Int. J. Pressure Vessel Technology*, **115**, 193-200.
- Eslami, M.R. and Alizadeh, S.H. (1990), “Galerkin finite element formulation of spherical shells under nonaxisymmetric loading”, *Proceedings of ASME PVP. Conf.*
- Eslami, M.R., Shakeri, M., Yas, M.H., and Ohadi, A.R. (1994), “Galerkin finite element of shells of revolution under blast loads”, *Proceedings of ASME/ESDA Conf.*, London.
- Eslami, M.R., Shakeri, M., Yas, M.H. and Barzekar, A.R. (0000), “A Galerkin finite element dynamic analysis of multilayered composite cylindrical shell”, under Review for publication.
- Heyliger, P.R. and Jilani, A. (1993), “Free vibrations of laminated anisotropic cylindrical shells”, *J. Engineering Mechanics*, **119**, 1062-1077.
- Hawkes, T.D. and Soldatos, K.P. (1992), “Three-dimensional axisymmetric vibrations of orthotropic and cross-ply laminated hollow cylinders”, *AIAA J.*, **30**, 1089-1098.
- Hung-Sying Jing and Kuan-Goang Tzeng (1993), “Approximate elasticity solution for laminated anisotropic finite cylinders”, *AIAA J.*, **31**, 2121-2129.
- Li, S. and Wang, X. (1986), “Elasticity solution for interlaminar stresses in a cross-ply laminated circular cylindrical shells”, *Proceeding of the Int. Symposium on composite materials and Struc.*, Lancaster, PA., 784-788.
- Liew, K.M. and Hung, K. (1995), “Three-dimensional vibratory characteristic of solid cylinder and some remark on simplified beam theories”, *J. Solid Structures*, **32**, 3499-3513.
- Pagano, N.J. (1969), “Exact solutions for composite laminates in cylindrical bending”, *J. Composite Materials*, **3**, 398-411.
- Pagano, N.J. and Hatfield, S.J. (1972), “Elastic behaviour of multilayered bidirectional composites”, *AIAA J.*, **10**, 931-933.
- Ren, J.G. (1987), “Exact solutions for laminated cylindrical shells in cylindrical bending”, *J. Composite Science and Technology*, **29**, 169.
- Soldatos, K.P. and Hadjigeorgiou, V.P. (1990), “Three-dimensional solution of the free vibration problem of homogeneous isotropic cylindrical shells and panels”, *J. Sound and Vibration*, **137**, 369-384.
- Soldatos, K.P. (1991), “A refined laminated plate and shell theory with applications”, *J. Sound and Vibration*, **144**, 109-129.
- Shakeri, M., Eslami, M.R., Fariborz, S. and Yas, M.H. (1996), “Analytical elasticity solution for laminated orthotropic cylindrical shell under impulse”, *Proceedings of Third APCOM Conf.*, 1591-1596.
- Shakeri, M., Eslami, M.R., and Yas, M.H. (1996), “Elasticity solution for laminated orthotropic cylindrical shells under dynamic local patch load”, *Proceedings of Third ASME/ESDAM Conf.*, Montpellier-France.
- Shakeri, M. and Yas, M.H. (1995), “Three-dimensional axisymmetric vibrations of orthotropic and cross-ply laminated hemispherical shells”, *Proceedings of 32th SES Conf.*, New-orlane America.
- Zhou, J. and Yang, B. (1995), “Three-dimensional analysis of simply supported laminated cylindrical shells with arbitrary thickness”, *AIAA J.*, **34**, 1960-1964.

## Notations

$h$	: thickness of cylindrical shell
$h_e$	: thickness of element
$h_k$	: thickness of $k$ th layer
$m$	: axial half-wave number
$t$	: time
$u_r$	: radial displacement
$u_x$	: axial displacement
$u_\theta$	: circumferential displacement

$C_{ij}$	: stiffness elastic constants
$L$	: length of cylindrical shell
$M$	: number of layers
$R$	: mean radius of cylindrical shell
$R_a$	: inner radius
$R_b$	: outer radius
$R_k$	: mean radius of $K$ th layer
$\varepsilon_{ij}, \gamma_{ij}$	: strain components
$\rho^k$	: density of $K$ th layer
$\sigma_{ij}, \tau_{ij}$	: stress components
$\omega$	: natural frequency

## Appendix

$$\begin{aligned}
k_{11} &= C_{33}^k (1/h_e - (r_j \ln(r_j/r_i)/h_e)) - C_{55}^k P_m h_e/3 - C_{22}^k (r_j/r_i h_e + 1/h_e - 2r_j/h_e^2 \ln(r_j/r_i)) \\
k_{12} &= -(C_{36}^k - C_{45}^k - C_{26}^k) P_m (r_j^2/h_e^2 \ln(r_j/r_i) + (r_i - 3r_j)/2h_e) + (C_{36}^k + C_{45}^k) P_m/2 \\
k_{13} &= -(C_{13}^k - C_{12}^k) P_m (r_j^2/h_e^2 \ln(r_j/r_i) + (r_i - 3r_j)/2h_e) + (C_{13}^k + C_{55}^k) P_m/2 \\
k_{14} &= C_{33}^k \left( \frac{r_j \ln r_j/r_i}{h_e^2} - 1/h_e \right) - C_{55}^k P_m^2 h_e/6 - C_{22}^k (-2h_e + (r_i + r_j)/h_e^2 \ln r_j/r_i) \\
k_{15} &= -(C_{36}^k - C_{45}^k - C_{26}^k) P_m ((r_i + r_j)/2h_e - r_j r_i/h_e^2 \ln r_j/r_i) - (C_{36}^k + C_{45}^k) P_m/2 \\
k_{16} &= -(C_{13}^k - C_{12}^k) P_m ((r_i + r_j)/2h_e - r_j r_i/h_e^2 \ln r_j/r_i) - (C_{13}^k + C_{55}^k) P_m/2 \\
k_{21} &= (2C_{45}^k + C_{26}^k) P_m (r_j^2/h_e^2 \ln r_j/r_i + (r_i - 3r_j)/2h_e) - (C_{45}^k + C_{36}^k) P_m/2 \\
k_{22} &= C_{44}^k (1/h_e - r_j \ln(r_j/r_i)/h_e^2) - C_{44}^k (r_j/r_i h_e + 1/h_e - 2r_j/h_e^2 \ln r_j/r_i) - P_m C_{66}^k h_e/3 \\
k_{23} &= 2C_{45}^k (1/h_e - r_j \ln r_j/r_i/h_e^2) - C_{16}^k P_m^2 h_e/3 \\
k_{24} &= (2C_{45}^k + C_{26}^k) P_m ((r_i + r_j)/2h_e - (r_j r_i/h_e^2) \ln r_j/r_i) + (C_{45}^k + C_{36}^k) P_m/2 \\
k_{25} &= C_{44}^k \left( \frac{r_j \ln r_j/r_i}{h_e^2} - 1/h_e \right) - C_{44}^k \left( -2h_e + \frac{r_j + r_i}{h_e^2} \ln r_j/r_i \right) - P_m^2 C_{66}^k h_e/6 \\
k_{26} &= 2C_{45}^k \left( \frac{r_j \ln r_j/r_i}{h_e^2} - 1/h_e \right) - C_{16}^k P_m^2 h_e/6 \\
k_{31} &= (C_{13}^k + C_{55}^k) P_m (r_j^2/h_e^2 \ln r_j/r_i + (r_i - 3r_j)/2h_e) - (C_{13}^k + C_{55}^k) P_m/2 \\
k_{32} &= -C_{16}^k P_m^2 h_e/3 \\
k_{33} &= -C_{11}^k P_m^2 h_e/3 + C_{55}^k (1/h_e - (r_j \ln r_j/r_i)/h_e^2) \\
k_{34} &= (C_{13}^k + C_{55}^k) P_m ((r_i + r_j)/2h_e - (r_j r_i/h_e^2) \ln r_j/r_i) + (C_{13}^k + C_{55}^k) P_m/2 \\
k_{35} &= -C_{16}^k P_m^2 h_e/6 \\
k_{36} &= -C_{11}^k P_m^2 h_e/6 + C_{55}^k ((r_j \ln r_j/r_i)/h_e^2 - 1/h_e) \\
k_{41} &= C_{33}^k (-1/h_e + (r_i/h_e^2) \ln r_j/r_i) - C_{55}^k P_m^2 h_e/6 - C_{22}^k ((r_j + r_i)/h_e^2) \ln r_j/r_i - 2/h_e \\
k_{42} &= -(C_{36}^k - C_{45}^k - C_{26}^k) P_m ((r_j + r_i)/2h_e - (r_j r_i/h_e^2) \ln r_j/r_i) + (C_{36}^k + C_{45}^k) P_m/2 \\
k_{43} &= -(C_{13}^k - C_{12}^k) P_m ((r_j + r_i)/2h_e - (r_j r_i/h_e^2) \ln r_j/r_i) + (C_{13}^k + C_{55}^k) P_m/2 \\
k_{44} &= C_{33}^k (1/h_e - (r_i/h_e^2) \ln r_j/r_i) - C_{55}^k P_m^2 h_e/3 - C_{22}^k (1/h_e + (r_i/h_e r_j) - (2r_i/h_e^2) \ln r_j/r_i) \\
k_{45} &= -(C_{36}^k - C_{45}^k - C_{26}^k) P_m ((r_j - 3r_i)/2h_e + (r_i^2/h_e^2) \ln r_j/r_i) - (C_{36}^k + C_{45}^k) P_m/2
\end{aligned}$$

$$\begin{aligned}
k_{46} &= -(C_{13}^k - C_{12}^k)P_m((r_j - 3r_i)2h_e + (r_i^2/h_e^2)\ln r_j/r_i) - (C_{13}^k + C_{55}^k)P_m/2 \\
k_{51} &= (2C_{45}^k + C_{26}^k)P_m((r_j + r_i)2h_e - (r_j r_i/h_e^2)\ln r_j/r_i) - (C_{45}^k + C_{36}^k)P_m/2 \\
k_{52} &= C_{44}^k(-1/h_e + (r_j/h_e^2)\ln r_j/r_i) - C_{44}^k(((r_j + r_i)/h_e^2)\ln r_j/r_i - 2/h_e) - C_{66}^k P_m^2 h_e/6 \\
k_{53} &= 2C_{45}^k(-1/h_e + (r_i/h_e^2)\ln r_j/r_i) - C_{16}^k P_m^2 h_e/6 \\
k_{54} &= (2C_{45}^k + C_{26}^k)P_m((r_j - 3r_i)2h_e + (r_i^2/h_e^2)\ln r_j/r_i) + (C_{45}^k + C_{36}^k)P_m/2 \\
k_{55} &= C_{44}^k(-r_i/h_e r_j + (r_i^2/h_e^2)\ln r_j/r_i) - C_{66}^k P_m^2 h_e/3 \\
k_{56} &= 2C_{45}^k(1/h_e - (r_i/h_e^2)\ln r_j/r_i) - C_{16}^k P_m^2 h_e/3 \\
k_{61} &= (C_{13}^k + C_{55}^k)P_m((r_j + r_i)2h_e - (r_j r_i/h_e^2)\ln r_j/r_i) - (C_{13}^k + C_{55}^k)P_m/2 \\
k_{62} &= -C_{16}^k P_m^2 h_e/6 \\
k_{63} &= -C_{11}^k P_m^2 h_e/6 + C_{55}^k(-1/h_e + r_i/h_e^2 \ln r_j/r_i) \\
k_{64} &= (C_{13}^k + C_{55}^k)P_m((r_j - 3r_i)2h_e + (r_i^2/h_e^2)\ln r_j/r_i) + (C_{13}^k + C_{55}^k)P_m/2 \\
k_{65} &= -C_{16}^k P_m^2 h_e/3 \\
k_{66} &= -C_{11}^k P_m h_e/3 + C_{55}^k(1/h_e - (r_i/h_e^2)\ln r_j/r_i) \\
M_{11} &= -\rho^k h_e/3 & M_{14} &= -\rho^k h_e/6 \\
M_{22} &= M_{33} = M_{44} = M_{55} = M_{66} = M_{11} & M_{25} &= M_{36} = M_{41} = M_{52} = M_{63} = M_{14} \\
A &= a_5 a_8 (a_{14} a_8 - a_7 a_{15}) \Delta_1 \\
B &= a_4 a_8 (a_{14} a_8 - a_7 a_{15}) \Delta_1 \\
C &= -a_9 a_3 (a_{14} a_8 - a_7 a_{15}) + (a_{10} a_8 + a_9 a_{15}) (a_2 a_8 - a_7 a_3) \Delta_1 \\
D &= -a_3 a_{12} (a_{14} a_8 - a_7 a_{15}) - (a_{12} a_8 - a_{12} a_{15}) (a_2 a_8 - a_7 a_3) \Delta_1 \\
E &= -a_8 a_3 (a_{14} a_8 - a_7 a_{15}) - (a_{17} a_8 + a_8 a_{15}) (a_2 a_8 - a_7 a_3) \Delta_1 \\
F &= a_{10} a_3 (a_{14} a_8 - a_7 a_{15}) - (a_{19} a_8 - a_{12} a_{15}) (a_2 a_8 - a_7 a_3) \Delta_1 \\
\Delta_1 &= (a_{18} a_8 - a_6 a_3) (a_{14} a_8 - a_7 a_{15}) - (a_{13} a_8 - a_6 a_{15}) (a_2 a_8 - a_7 a_3) \\
A' &= a_5 a_8 (a_{13} a_8 - a_6 a_{15}) \Delta' \\
B' &= a_4 a_8 (a_{13} a_8 - a_6 a_{15}) \Delta' \\
C' &= -a_9 a_3 (a_{18} a_8 - a_6 a_{15}) - (a_{10} a_8 - a_9 a_{15}) (a_1 a_8 - a_6 a_3) \Delta' \\
D' &= -a_{12} a_3 (a_{13} a_8 - a_6 a_{15}) - (a_{12} a_8 - a_{11} a_{15}) (a_1 a_8 - a_6 a_3) \Delta' \\
E' &= -a_8 a_3 (a_{14} a_8 - a_7 a_{15}) - (a_{17} a_8 + a_8 a_{15}) (a_2 a_8 - a_7 a_3) \Delta' \\
F' &= -a_{12} a_3 (a_{13} a_8 - a_6 a_{15}) - (a_{19} a_8 - a_{12} a_{15}) (a_1 a_8 - a_6 a_3) \Delta' \\
\Delta' &= (a_2 a_8 - a_7 a_3) (a_{13} a_8 - a_6 a_{15}) - (a_1 a_8 - a_6 a_3) (a_{14} a_8 - a_7 a_{15}) \\
A'' &= a_5 a_6 (a_{14} a_6 - a_7 a_{13}) \Delta'' \\
B'' &= a_4 a_6 (a_{14} a_6 - a_7 a_{13}) \Delta'' \\
C'' &= -a_9 a_1 (a_{14} a_6 - a_7 a_{13}) + (a_{10} a_6 + a_9 a_{13}) (a_2 a_6 - a_7 a_1) \Delta'' \\
D'' &= -a_9 a_1 (a_{14} a_6 - a_7 a_{13}) - (a_{12} a_6 - a_{11} a_{13}) (a_2 a_6 - a_7 a_1) \Delta'' \\
E'' &= -a_8 a_1 (a_{14} a_6 - a_7 a_{13}) + (a_{17} a_6 + a_8 a_{13}) (a_2 a_6 - a_7 a_1) \Delta'' \\
F'' &= -a_{12} a_1 (a_{14} a_6 - a_7 a_{13}) - (a_{19} a_6 - a_{12} a_{13}) (a_2 a_6 - a_7 a_1) \Delta'' \\
\Delta'' &= (a_3 a_6 - a_8 a_1) (a_{14} a_6 - a_7 a_{13}) - (a_2 a_6 - a_7 a_1) (a_{15} a_6 - a_8 a_{13}) \\
a_1 &= C_{23}^k (\Sigma h_e + R_i) + C_{33}^k / h_e - C_{23}^{k+1} (\Sigma h_e + R_i) + C_{33}^{k+1} h_e \\
a_2 &= (-C_{36}^k + C_{13}^{k+1}) P_m \\
a_3 &= (-C_{13}^k + C_{13}^{k+1}) P_m \\
a_4 &= C_{33}^{k+1} / h_e & a_5 &= C_{33}^k / h_e & a_6 &= (C_{45}^k - C_{45}^{k+1}) P_m \\
a_7 &= C_{44}^k (-1/h_e + R_i) + 1/h_e + C_{44}^{k+1} (1/h_e + R_i) + 1/h_e \\
a_8 &= C_{45}^k / h_e + C_{45}^{k+1} h_e & a_9 &= C_{44}^k / h_e & a_{10} &= C_{45}^{k+1} / h_e & a_{11} &= C_{44}^{k+1} / h_e
\end{aligned}$$

$$\begin{aligned}
 a_{12} &= C_{45}^{k+1}/h_e & a_{13} &= (C_{55}^k - C_{55}^{k+1})P_m \\
 a_{14} &= C_{45}^k(-1(\Sigma h_e + R_i) + 1/h_e) + C_{45}^{k+1}(1(\Sigma h_e + R_i) + 1/h_e) \\
 a_{15} &= (C_{55}^k/h_e + C_{55}^{k+1}/h_e) & a_{16} &= -C_{45}^k/h_e & a_{17} &= -C_{55}^k/h_e \\
 a_{18} &= C_{45}^{k+1}/h_e & a_{19} &= C_{55}^{k+1}/h_e \\
 M'_{11} &= -\rho^k h_e/3 - \rho^k h_e/6 A & M'_{12} &= -\rho^k h_e/6 C & M'_{13} &= -\rho^k h_e/6 E \\
 M'_{14} &= -\rho^k h_e/6 B & M'_{15} &= -\rho^k h_e/6 S & M'_{16} &= -\rho^k h_e/6 F \\
 M'_{21} &= -\rho^k h_e/6 A' & M'_{22} &= -\rho^k h_e/3 - \rho h_e/6 C' & M'_{23} &= -\rho^k h_e/6 E' \\
 M'_{24} &= -\rho^k h_e/6 B' & M'_{25} &= -\rho^k h_e/6 D' & M'_{26} &= -\rho^k h_e/6 F' \\
 M'_{31} &= -\rho^k h_e/6 A'' & M'_{32} &= -\rho^k h_e/6 C'' & M'_{33} &= -\rho^k h_e/3 - \rho^k h_e/6 E'' \\
 M'_{34} &= -\rho^k h_e/6 B'' & M'_{35} &= -\rho^k h_e/6 D'' & M'_{36} &= -\rho^k h_e/6 F'' \\
 M'_{41} &= -\rho^k h_e/6 - \rho^k h_e/3 A & M'_{42} &= -\rho^k h_e/3 C & M'_{43} &= -\rho^k h_e/3 E \\
 M'_{44} &= -\rho^k h_e/6 B & M'_{45} &= -\rho^k h_e/3 D & M'_{46} &= -\rho^k h_e/3 F \\
 M'_{51} &= -\rho^k h_e/3 A' & M'_{52} &= -\rho^k h_e/6 - \rho^k h_e/3 C' & M'_{53} &= -\rho^k h_e/3 E' \\
 M'_{54} &= -\rho^k h_e/3 B' & M'_{55} &= -\rho^k h_e/3 D' & M'_{56} &= -\rho^k h_e/3 F' \\
 M'_{61} &= -\rho^k h_e/3 A'' & M'_{62} &= -\rho^k h_e/3 C'' & M'_{63} &= -\rho^k h_e/6 - \rho^k h_e/3 E'' \\
 M'_{64} &= -\rho^k h_e/3 B'' & M'_{65} &= -\rho^k h_e/6 D'' & M'_{66} &= -\rho^k h_e/3 F'' \\
 k'_{11} &= k_{11} + k_{14}A + k_{15}A' + k_{16}A'' & k'_{12} &= k_{12} + k_{14}C + k_{15}C' + k_{16}C'' \\
 k'_{13} &= k_{13} + k_{14}E + k_{15}E' + k_{16}E'' & k'_{14} &= k_{14}B + k_{15}B' + k_{16}B'' \\
 k'_{15} &= k_{14}D + k_{15}D' + k_{16}D'' & k'_{16} &= k_{14}F + k_{15}F' + k_{16}F'' \\
 k'_{21} &= k_{21} + k_{24}A + k_{25}A' + k_{26}A'' & k'_{22} &= k_{22} + k_{24}C + k_{25}C' + k_{26}C'' \\
 k'_{23} &= k_{23} + k_{24}E + k_{25}E' + k_{26}E'' & k'_{24} &= k_{24}B + k_{25}B' + k_{26}B'' \\
 k'_{25} &= k_{24}D + k_{25}D' + k_{26}D'' & k'_{26} &= k_{24}F + k_{25}F' + k_{26}F'' \\
 k'_{31} &= k_{31} + k_{34}A + k_{35}A' + k_{36}A'' & k'_{32} &= k_{32} + k_{34}C + k_{35}C' + k_{36}C'' \\
 k'_{33} &= k_{33} + k_{34}E + k_{35}E' + k_{36}E'' & k'_{34} &= k_{34}B + k_{35}B' + k_{36}B'' \\
 k'_{35} &= k_{34}D + k_{35}D' + k_{36}D'' & k'_{36} &= k_{34}F + k_{35}F' + k_{36}F'' \\
 k'_{41} &= k_{41} + k_{44}A + k_{45}A' + k_{46}A'' & k'_{42} &= k_{42} + k_{44}C + k_{45}C' + k_{46}C'' \\
 k'_{43} &= k_{43} + k_{44}E + k_{45}E' + k_{46}E'' & k'_{44} &= k_{44}B + k_{45}B' + k_{46}B'' \\
 k'_{45} &= k_{44}D + k_{45}D' + k_{46}D'' & k'_{46} &= k_{44}F + k_{45}F' + k_{46}F'' \\
 k'_{51} &= k_{51} + k_{54}A + k_{55}A' + k_{56}A'' & k'_{52} &= k_{52} + k_{54}C + k_{55}C' + k_{56}C'' \\
 k'_{53} &= k_{53} + k_{54}E + k_{55}E' + k_{56}E'' & k'_{54} &= k_{54}B + k_{55}B' + k_{56}B'' \\
 k'_{55} &= k_{54}D + k_{55}D' + k_{56}D'' & k'_{56} &= k_{54}F + k_{55}F' + k_{56}F'' \\
 k'_{61} &= k_{61} + k_{64}A + k_{65}A' + k_{66}A'' & k'_{62} &= k_{62} + k_{64}C + k_{65}C' + k_{66}C'' \\
 k'_{63} &= k_{63} + k_{64}E + k_{65}E' + k_{66}E'' & k'_{64} &= k_{64}B + k_{65}B' + k_{66}B'' \\
 k'_{65} &= k_{64}D + k_{65}D' + k_{66}D'' & k'_{66} &= k_{64}F + k_{65}F' + k_{66}F'' \\
 M''_{11} &= -\rho^{k+1}h_e/3 A & M''_{12} &= -\rho^{k+1}h_e/3 C & M''_{13} &= -\rho^{k+1}h_e/3 E \\
 M''_{14} &= -\rho^{k+1}h_e/6 - \rho^{k+1}h_e/3 B & M''_{15} &= -\rho^{k+1}h_e/3 D & M''_{16} &= -\rho^{k+1}h_e/3 F \\
 M''_{21} &= -\rho^{k+1}h_e/3 A' & M''_{22} &= -\rho^{k+1}h_e/3 C' & M''_{23} &= -\rho^{k+1}h_e/3 E' \\
 M''_{24} &= -\rho^{k+1}h_e/3 B' & M''_{25} &= -\rho^{k+1}h_e/6 - \rho h_e/3 D' & M''_{26} &= -\rho^{k+1}h_e/3 F' \\
 M''_{31} &= -\rho^{k+1}h_e/3 A'' & M''_{32} &= -\rho^{k+1}h_e/3 C'' & M''_{33} &= -\rho^{k+1}h_e/3 E'' \\
 M''_{34} &= -\rho^{k+1}h_e/3 B'' & M''_{35} &= -\rho^{k+1}h_e/3 D'' & M''_{36} &= -\rho^{k+1}h_e/6 - \rho^{k+1}h_e/3 F'' \\
 M''_{41} &= -\rho^{k+1}h_e/6 A & M''_{42} &= -\rho^{k+1}h_e/6 C & M''_{43} &= -\rho^{k+1}h_e/6 E \\
 M''_{44} &= -\rho^{k+1}h_e/6 - \rho^{k+1}h_e/3 B & M''_{45} &= -\rho^{k+1}h_e/6 D & M''_{46} &= -\rho^{k+1}h_e/6 F
 \end{aligned}$$

$$\begin{aligned}
M''_{51} &= -\rho^{k+1}h_e/6 A' & M''_{52} &= -\rho^{k+1}h_e/6 C' & M''_{53} &= -\rho^{k+1}h_e/6 E' \\
M''_{54} &= -\rho^{k+1}h_e/6 B' & M''_{55} &= -\rho^{k+1}h_e/6 - \rho h_e/3 D' & M''_{56} &= -\rho^{k+1}h_e/6 F' \\
M''_{61} &= -\rho^{k+1}h_e/6 A'' & M''_{62} &= -\rho^{k+1}h_e/6 C'' & M''_{63} &= -\rho^{k+1}h_e/6 E'' \\
M''_{64} &= -\rho^{k+1}h_e/6 B'' & M''_{65} &= -\rho^{k+1}h_e/6 D'' & M''_{66} &= -\rho^{k+1}h_e/6 - \rho^{k+1}h_e/3 F'' \\
k''_{11} &= k_{11}A + k_{12}A' + k_{13}A'' & k''_{12} &= k_{11}C + k_{12}C' + k_{13}C'' \\
k''_{13} &= k_{11}E + k_{12}E' + k_{13}E'' & k''_{14} &= k_{14} + k_{11}B + k_{12}B' + k_{13}B'' \\
k''_{15} &= k_{15} + k_{11}D + k_{12}D' + k_{13}D'' & k''_{16} &= k_{16} + k_{11}F + k_{12}F' + k_{13}F'' \\
k''_{21} &= k_{21}A + k_{22}A' + k_{23}A'' & k''_{22} &= k_{21}C + k_{22}C' + k_{23}C'' \\
k''_{23} &= k_{21}E + k_{22}E' + k_{23}E'' & k''_{24} &= k_{24} + k_{21}B + k_{22}B' + k_{23}B'' \\
k''_{25} &= k_{25} + k_{21}D + k_{22}D' + k_{23}D'' & k''_{26} &= k_{26} + k_{21}F + k_{22}F' + k_{23}F'' \\
k''_{31} &= k_{31}A + k_{32}A' + k_{33}A'' & k''_{32} &= k_{31}C + k_{32}C' + k_{33}C'' \\
k''_{33} &= k_{31}E + k_{32}E' + k_{33}E'' & k''_{34} &= k_{34} + k_{31}B + k_{32}B' + k_{33}B'' \\
k''_{35} &= k_{35} + k_{31}D + k_{32}D' + k_{33}D'' & k''_{36} &= k_{36} + k_{31}F + k_{32}F' + k_{33}F'' \\
k''_{41} &= k_{41}A + k_{42}A' + k_{43}A'' & k''_{42} &= k_{41}C + k_{42}C' + k_{43}C'' \\
k''_{43} &= k_{41}E + k_{42}E' + k_{43}E'' & k''_{44} &= k_{44} + k_{41}B + k_{42}B' + k_{43}B'' \\
k''_{45} &= k_{45} + k_{41}D + k_{42}D' + k_{43}D'' & k''_{46} &= k_{46} + k_{41}F + k_{42}F' + k_{43}F'' \\
k''_{51} &= k_{51}A + k_{52}A' + k_{53}A'' & k''_{52} &= k_{51}C + k_{52}C' + k_{53}C'' \\
k''_{53} &= k_{51}E + k_{52}E' + k_{53}E'' & k''_{54} &= k_{54} + k_{51}B + k_{52}B' + k_{53}B'' \\
k''_{55} &= k_{55} + k_{51}D + k_{52}D' + k_{53}D'' & k''_{56} &= k_{56} + k_{51}F + k_{52}F' + k_{53}F'' \\
k''_{61} &= k_{61}A + k_{62}A' + k_{63}A'' & k''_{62} &= k_{61}C + k_{62}C' + k_{63}C'' \\
k''_{63} &= k_{61}E + k_{62}E' + k_{63}E'' & k''_{64} &= k_{64} + k_{61}B + k_{62}B' + k_{63}B'' \\
k''_{65} &= k_{65} + k_{61}D + k_{62}D' + k_{63}D'' & k''_{66} &= k_{66} + k_{61}F + k_{62}F' + k_{63}F''
\end{aligned}$$